Environment Protection Engineering

Vol. 49 2023 No. 3

DOI: 10.37190/epe230306

ZHENGCHENG WEN [1], XIAOFENG ZHANG[1], JU HUANG[1], ZHENGYIN YANG[1]

NUMERICAL SIMULATION STUDY ON NO OXIDATION BY ˙OH RADICAL CLUSTERS IN FLUE GAS

Fenton reaction is an important method to remove NO from flue gas. ˙OH radicals generated in the Fenton reaction can effectively oxidize NO to NO_2, which is absorbed and removed by alkali sorbent. To supply guidance for engineering research, numerical simulation of NO oxidation by ˙OH radical clusters in flue gas has been carried out using Fluent software. The average concentration of NO on the cross sections at various positions of a cylindrical pipe with a circular surface was calculated by simulation. Under various working conditions (temperature, ˙OH/NO molar ratio, NO concentration in flue gas, and jet velocity), NO oxidation efficiency by ˙OH radical was simulated and the key factors affecting NO oxidation were analyzed. The results show that temperature and ˙OH/NO molar ratio are the key factors affecting the oxidation of NO by ˙OH radicals. The injection velocity has also a significant effect on the oxidation efficiency while the moisture and oxygen content are minor factors influencing the process. The optimum oxidation efficiency of NO is obtained at 473–523 K, the molar ratio of ˙OH/NO ca. 1.4, the jet velocity 10 m/s, and the flue gas velocity of 3 m/s.

1. INTRODUCTION

In recent years, biomass has attracted more and more attention because of its rich resources, less pollution, and environmental friendliness. The amount of carbon dioxide absorbed by biomass through photosynthesis is equal to the amount released by its complete combustion, which realizes zero emission of carbon dioxide from the root and is the fundamental method to solve the greenhouse effect and global warming [1]. The government report also points out that promoting biomass power generation, including coal-fired coupled biomass power generation, is an important means to achieve the goal of “double carbon”. However, like coal burning, biomass power generation produces many air pollutants, and nitrogen oxides (NO_x) being one of them. Nitrogen oxides are

[1]College of Science, Hangzhou Dianzi University, Hangzhou, China, 310018, corresponding author Z. Wen, email address: wenzc@hdu.edu.cn

extremely harmful: in the atmosphere, they form acid rain and acid mist, which destroy the ecological environment [2, 3], and also form photochemical smog, destroying the ozone layer, causing global warming, etc. [4–6]. The presence of NO_x not only causes extremely serious pollution and destruction to the ecological environment but also direct or indirect harm and influence on human health [7]. Therefore, it is extremely important to control and treat the emission of nitrogen oxides.

NO is an important component of nitrogen oxides. For NO removal, selective non-catalytic reduction (SNCR) and selective catalytic reduction (SCR) technologies are currently the mainstream technologies. The reaction temperature of SNCR is demanding, and the nitrogen removal efficiency is not high enough [8]. Although the removal efficiency of SCR technology is improved compared with SNCR technology, there are still some problems such as high catalyst cost and pollution caused by ammonia leakage [9, 10]. $NaClO_2$ oxidation and potassium permanganate oxidation have high oxidation removal efficiency for NO, but $NaClO_2$ requires high corrosion resistance of equipment, and the price of the oxidant is relatively high, which restricts its industrial application [11]. The preparation of $KMnO_4$ is complex and expensive, and the manganese dioxide precipitate generated in the reaction process causes equipment blockage [12], so the application of this process in industrial boilers is also limited.

The Fenton method is an advanced oxidation denitrification method, which has the advantages of simple operation, fast reaction, no pollution, and high oxidation efficiency. It is considered one of the most promising oxidation methods in advanced oxidation technology at present [13, 14]. Fenton technology uses Fe^{2+} ion as a catalyst and H_2O_2 as an oxidant. H_2O_2 is activated and decomposed into ˙OH radicals by electron transfer between Fe^{2+} and H_2O_2, which can oxidize NO to form NO_2 and then remove it [15]. Cui et al. used Fe/ZSM-5 to catalyze the oxidation of NO by hydrogen peroxide; the removal efficiency of NO reached 90% [16]. Song et al., employed gas-phase heterogeneous Fenton-like technology to remove NO and SO_2 at a fixed bed, and $Fe_{2.5}Cu_{0.5}O_4$ is the most prominent catalyst. Its removal efficiency reached 94.1% and 100%, respectively [17]; Wen et al. doped Fenton catalyst and combined it with a hydrogen peroxide atomization device to remove NO from flue gas. Under optimal conditions, the removal efficiency of 15% Fe_2O_3+15% C_eO_2/Al_2O_3 catalyst for NO can reach 90% [18]. In this paper, the computational fluid dynamics (CFD) method by means of FLUENT software was used to simulate the oxidation of NO by ˙OH radicals in a flue gas environment. The key factors affecting oxidation efficiency have been analyzed to provide a reference for practical engineering applications.

2. SIMULATION METHOD

Establishment of FLUENT model. To simulate the distribution of NO and the oxidation efficiency of ˙OH radicals, it was necessary to establish the corresponding model

and grid division. In the model, a cylindrical pipe 10 m long, and 2 m in diameter was used. To improve mixing ˙OH radicals with flue gas, 19 small round openings 0.1 m in diameter were placed on the bottom of the cylinder as the incident surface of ˙OH radical jet, while the rest are used as the exhaust gas inlet. The distribution of the incident ports of the whole pipe model is shown in Fig. 1a.

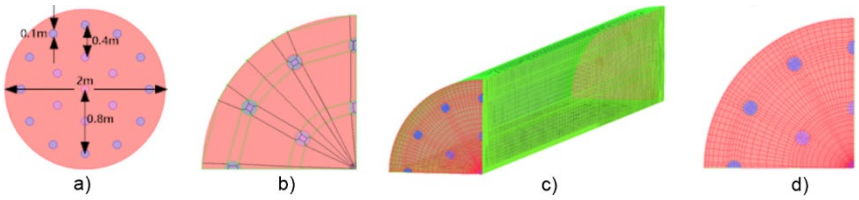

Fig. 1. Model setup and grid drawing: a) bottom of the pipe, b) edge of the pipe, c) mesh, d) mesh of the bottom

To improve the accuracy and efficiency of the subsequent calculation, the whole cylindrical pipe was cut symmetrically, into four equal parts. The NO distribution and oxidation in each of the four parts were studied separately, and the cutting plane was a symmetrical plane, which did not affect the subsequent simulation calculation.

Grid rendering. The whole grid was drawn by ANSYS-ICEM CFD software. The hexahedral mesh was drawn by an O-block structured mesh. To meet the design needs of the pipeline, it was necessary to make some specific constraints on the edge of the block and the jet inlet. The edge at the bottom of the block is shown in Fig. 1b. The green edge shows that it has been fixed with a certain curve to form constraints, while the black edge shows the separation between ordinary blocks on the model surface without specific constraints. In this way, the jet inlet and the flue gas inlet can be divided by the body and the edge, and the boundary settings of the pipe wall, symmetry plane, and outlet can be completed. After building the block, the mesh of the model can be generated by setting the overall mesh size. Then, the grid was optimized and leveled. It is shown in Fig. 1c, and the pipeline bottom grid is shown in Fig. 1d.

Grid quality inspection. The total number of meshes in this model is 301 694 by ANSYS-ICEM CFD software. The common mesh quality detects the deformation degree of the unit mesh hexahedron by calculating the ratio of the minimum value to the maximum value of the Jacobian determinant of the unit mesh hexahedron (Jacobian ratio). It is generally considered that the closer to 1, the better the mesh quality is. In addition, it is common to judge the mesh quality by calculating the distortion and collapse values of the three-dimensional mesh [19]. The evaluation criterion we adopt is to calculate the Jacobian ratio. The minimum mesh quality of the model is 0.415, the optimum mesh quality is 1, about 80% of the mesh quality is greater than 0.8, and the

average mesh quality is 0.897. Therefore, this grid can meet the needs of calculation, ensure the convergence of calculation, and get accurate results.

Fluent solver settings. To simulate the distribution and degradation of pollutants in the pipeline within 10 s, the FLUENT calculation model was chosen as a transient model with 1000 time-steps, each lasting 0.01 s. To ensure that each step can achieve convergence, the maximum number of iterations under each time step was selected. The influence of gravitational acceleration was ignored, and because chemical reactions are involved, the energy equation was considered. A possible k-ε model is the turbulence model. Compared with the standard k-ε model, its advantage is that it can keep the Reynolds stress consistent with the real turbulence and can simulate the diffusion velocity of the plane and round hole jet more accurately. The component transport model is selected and imported into the CHEMKIN reaction mechanism and thermodynamics documents [20, 21]. The finite-rate model (finite-rate/no TCI) was adopted, because the chemical reaction between components was involved, and volume reaction and inlet diffusion between components were checked. The jet inlet and exhaust gas inlet were set as velocity inlets, the pipeline outlet was pressure outlet, the pipeline wall was selected as a non-slip wall, the inter was selected as symmetry plane, the standard initialization was adopted, all-zone was selected, and the corresponding components and initial temperature were set.

Observation surface setting. The observation surface was along the height of the pipeline. The cross sections for monitoring NO concentration and surface standard deviation were set every 1 m. Data were recorded every 50 time steps. This observation surface can be used for monitoring the degradation efficiency and uniformity of waste gas with the increase in distance. At the same time, another observation surface was established along the pipeline section to record data every 50 time steps. This observation surface can be used to check the gas diffusion

$$E_f = \frac{C_{\text{in}} - C_{\text{out}}}{C_{\text{in}}} \times 100\%$$

where E_f is the oxidation efficiency of NO, C_{in} and C_{out} are the concentrations of NO at the inlet and outlet of flue gas, ppm.

3. RESULTS AND DISCUSSION

3.1. POLLUTANTS' DISTRIBUTION OF ·OH RADICALS

Firstly, the distribution of pollutants is simulated. The inlet gas parameters are as follows: exhaust gas inlet velocity 3 m/s, temperature is 473 K, input components: nitrogen 77.99%, carbon dioxide 12%, oxygen 5%, water 5% and nitric oxide 0.01%

(100 ppm). Jet inlet: the velocity is 10 m/s and the temperature is 473 K. The inputs are nitrogen 78.986%, oxygen 21% and ˙OH 0.014% (140 ppm). The molar average value of NO was monitored at intervals of 1 m.

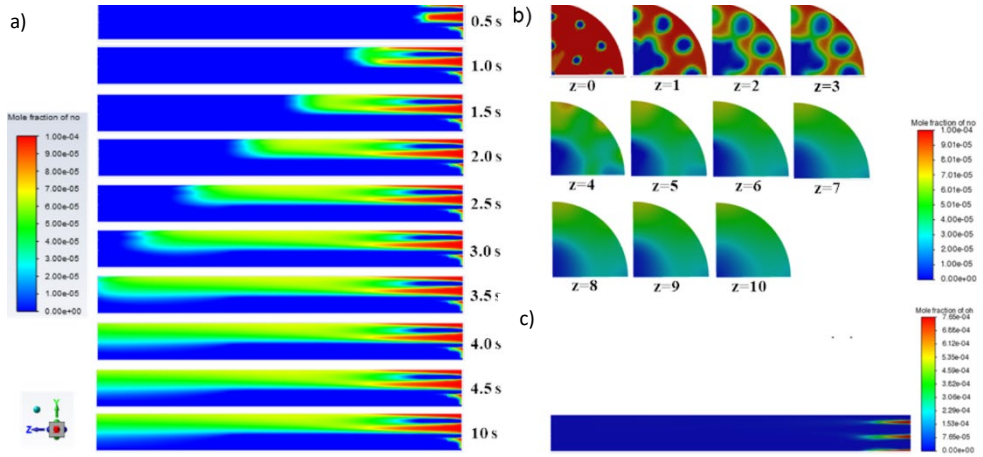

Fig. 2. NO concentration distribution in the pipeline section and its cross section:
a) distribution and concentration of NO in the pipeline section depending on time,
b) distribution and concentration of NO in the cross section of the pipe at 10 s,
c) distribution and concentration of ˙OH radicals in the pipeline profile at 10 s

The oxidation of NO by ˙OH radicals mainly occurs in the first 5 s (Fig. 2a). In 10 s, the gas distribution in the pipeline is basically stable, and the gas molar concentration no longer changes in a large range with time. The oxidation efficiency of ˙OH to NO can be reflected by measuring the average NO concentration in the cross-section of the pipeline.

The nephogram color in Fig. 2b suggests the molar concentration of NO gas. The closer its color is to red, the higher the NO concentration at this cross-section is. The closer the color is to blue, the lower the NO concentration is. In the range of 0–5 m, the NO concentration gradually decreases with the increase in distance. By comparing the distribution of pollutants in the cross-section and section of the pipeline, it can be seen that the distribution of NO in the middle of the pipeline is relatively uniform, and the distribution in the back section of the pipeline is basically stable.

From Fig. 2c, we can get the distribution and molar concentration of ˙OH radicals in the pipeline section. The farther away from the jet inlet, the lower the concentration of ˙OH radicals is. The NO distribution in the gas in the second half of the pipeline is uniform and stable. Therefore, the NO concentration can measure the oxidation efficiency of ˙OH radicals to NO. The comparison of oxidation efficiency in the latter part of the pipeline is usually based on the oxidation efficiency in the second half of the

pipeline. For more convenience, the oxidation efficiency at the outlet of the pipeline is compared.

3.2. FACTORS AFFECTING THE OXIDATION EFFICIENCY OF NO BY ˙OH RADICALS

According to the preliminary conclusions, the working conditions of oxidizing NO with various ˙OH radicals were simulated. Under various ambient temperatures, ˙OH/NO molar ratio, NO concentration in flue gas, jet velocity, water and oxygen concentration in flue gas, the oxidation of NO by ˙OH radicals were studied, and the optimum working conditions of NO oxidation by ˙OH radicals were found.

Effect of temperature. The inlet velocity of exhaust gas was 3 m/s, the concentration of NO 100 ppm, the molar fraction of carbon dioxide 12%, the molar fraction of oxygen 5%, the molar fraction of water 5%, the jet flow velocity 10 m/s, the molar ratio of OH/NO 1.2:1. N_2 was used as inert gas, the gas temperature of the waste inlet and the jet inlet was changed at 50 K intervals, and the oxidation efficiency of ˙OH radicals oxidizing NO at various temperatureswas simulated.

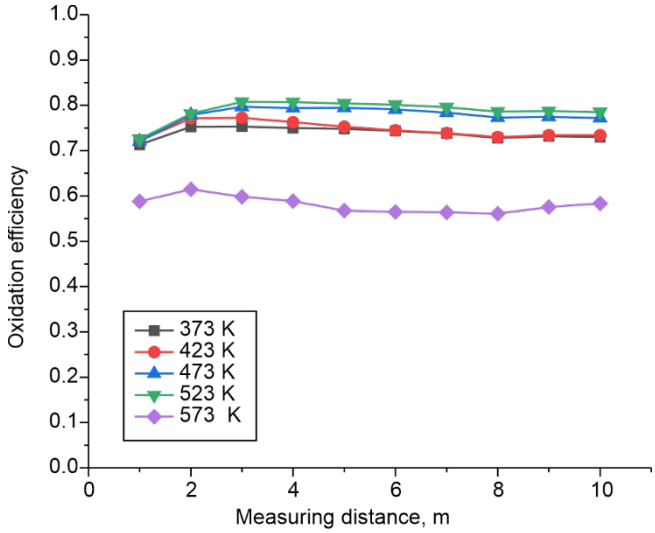

Fig. 3. Oxidation efficiency of NO at various temperatures

As can be seen in Fig. 3, in the range from 373 K to 523 K, with the increase of temperature the oxidation efficiency of ˙OH to NO also shows an upward trend, but the oxidation efficiency increases obviously from 73 to 77% at 473 K, but it does not increase significantly in the temperature ranges of 373–423 K and 473–523 K. On the whole, the influence of ˙OH radicals on the oxidation efficiency of NO is not particularly

strong in the temperature range of 373–523 K. However, over 573 K, the oxidation efficiency is reduced from 78% at 523 K to 58%. CHEMKIN software was used to analyze the sensitivity of NO under these two working conditions, as shown in Fig. 4.

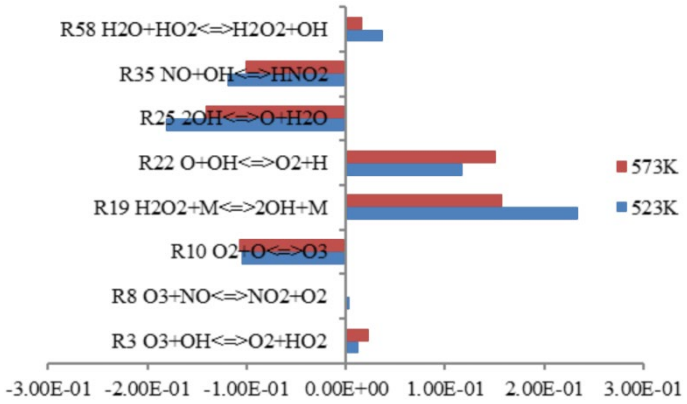

Fig. 4. Comparison diagram of sensitivity analysis of NO at various temperatures

Eight elementary reactions have great influence on NO oxidation, and the larger the sensitivity coefficient value, the greater the influence of this reaction on NO is. The sensitivity of R19 and R22 is positive under these two conditions, which means that these two reactions promote the formation of NO, while the sensitivity of other reactions is negative under these two conditions, which means that the other reactions inhibit the formation of NO. As shown in Fig. 4, by comparing the sensitivity of O + ˙OH = O_2 + H reaction at two temperatures, it can be seen that the sensitivity of the reaction has been strengthened with the increase of temperature, and the sensitivity coefficient of the reaction is positive, indicating that the reaction plays a catalytic role in the production of NO, that is, compared with 523 K, it has a stronger catalytic role in the production of NO at 573 K. Thus, the oxidation efficiency of NO is inhibited. Although higher temperature decreases the sensitivity of the elementary reaction R19 that promotes NO production, it also decreases the sensitivity of the elementary reactions R25 and R35 that inhibit NO production. Compared with the whole, the oxidation efficiency of NO is reduced at higher temperatures.

Effect of molar ratio of OH/NO. The inlet velocity of exhaust gas was 3 m/s, the concentration of NO 100 ppm, the molar fraction of carbon dioxide 12%, the molar fraction of oxygen 5%, the molar fraction of water 5%, the jet velocity 10 m/s, the temperature 473 K, N_2 was used as the inert gas, the molar ratio of ˙OH/NO changed, and the oxidation efficiency of NO to ˙OH radicals was simulated under various molar ratios of ˙OH/NO. The measurement time point is 10 s.

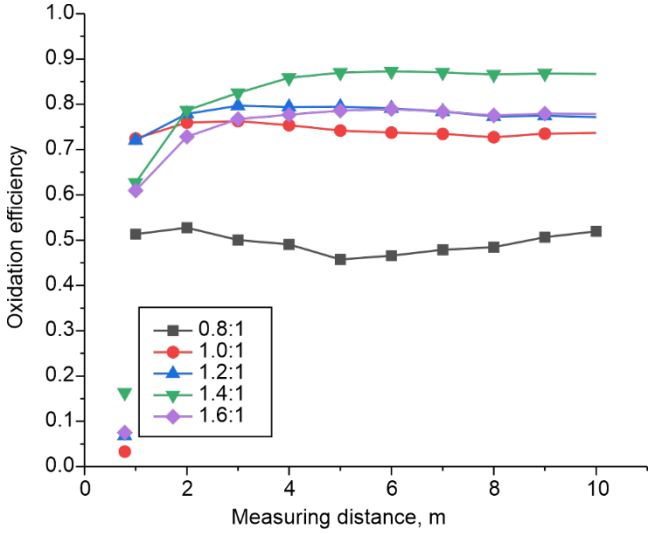

Fig. 5. Oxidation efficiency of NO under various molar ratios of ˙OH/NO

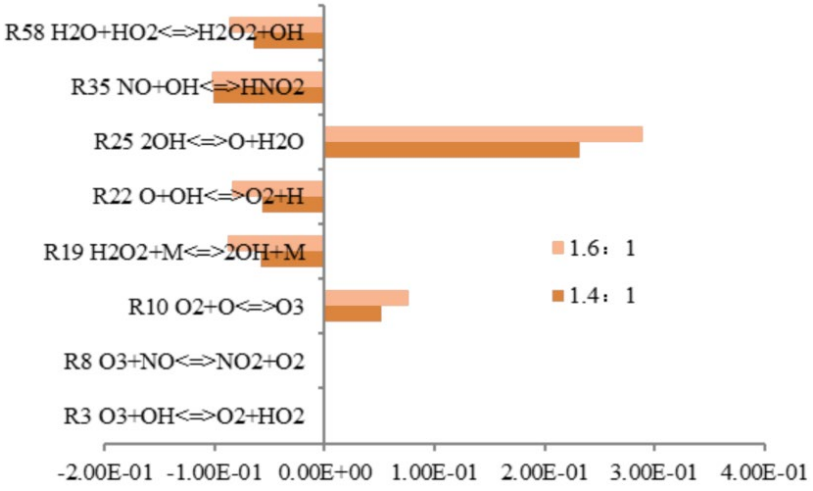

Fig. 6. Comparison chart of sensitivity analysis of NO under various ˙OH/NO concentrations

It can be seen from Fig. 5 that in the range of ˙OH/NO molar ratios from 0.8 to 1.4, with the increase of molar ratio, the oxidation efficiency of ˙OH radicals was also continuously improved, and when the molar ratio was 1.0, the oxidation efficiency was particularly obvious compared with the case when the molar ratio was 0.8, which was about 22% higher. However, when the molar ratio reached 1.6, the oxidation efficiency decreased from 87% at a molar ratio of 1.4 to 78%. As can be seen from the sensitivity analysis of Fig. 6, the reason for this result may be that the presence of high concentration of ˙OH radicals in the

pipeline further enhances the reaction rate of 2˙OH = O + H_2O, and increases the consumption of ˙OH radicals, but has NO promotion effect on NO oxidation reaction, resulting in further reduction of ˙OH radicals, thus reducing its oxidation efficiency.

Effect of initial concentration of NO. The inlet velocity of exhaust gas was 3 m/s, the molar fraction of carbon dioxide 12%, the molar fraction of oxygen 5%, the molar fraction of water 5%, the jet velocity 10 m/s, at 473 K, the molar ratio of ˙OH/NO was 1.4, N_2 was used as an inert gas, the initial concentration of NO was changed from 100 ppm to 200 ppm, the interval was 25 ppm every time, the oxidation efficiency of NO to ˙OH radicals was simulated under various initial concentrations of NO, and the measurement time was 10 s.

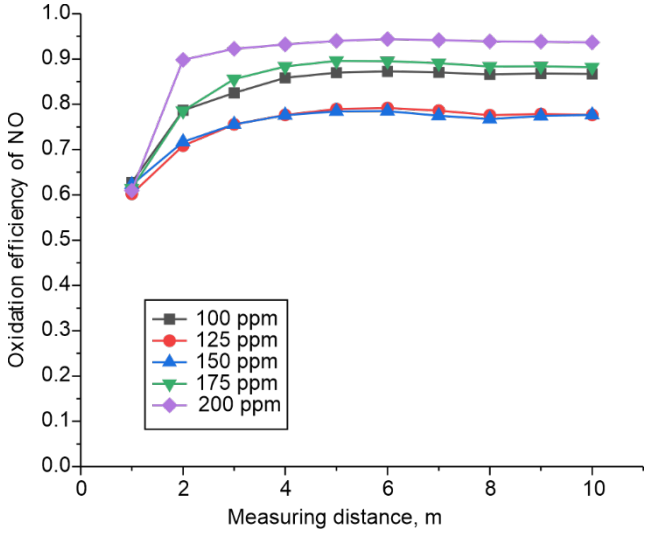

Fig. 7. Oxidation efficiency of NO under various initial NO concentrations

In the initial concentration range of NO from 100 ppm to 200 ppm, the oxidation of NO by ˙OH radicals was not subject to obvious rules, but they all had high oxidation efficiency, reaching about 80% or more (Fig. 7). The oxidation reaction was more efficient when the concentration of NO was 175 ppm and 200 ppm, and its efficiency reached 93.7% when the concentration of NO was 200 ppm. Therefore, it seemed that when the initial concentration of NO in flue gas was high, a better oxidation effect could be obtained. After all, a high concentration of NO can increase the contact frequency between ˙OH radicals and NO, which makes the oxidation reaction more probable.

Effect of jet velocity. The inlet velocity of exhaust gas was 3 m/s, the concentration of NO 100 ppm, the molar fraction of carbon dioxide 12%, the molar fraction of oxygen

5%, the molar fraction of water was 5%, the temperature was 473 K, the molar ratio of ˙OH/NO was 1.4, N_2 was used as inert gas, the incident velocity of the inlet gas of jet was changed, and the oxidation efficiency of ˙OH radicals by NO was simulated at the jet velocity. The measurement time point was 10 s.

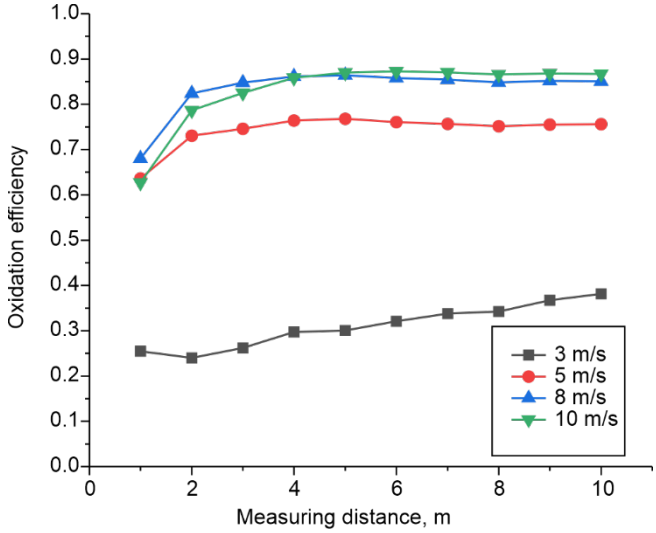

Fig. 8. Oxidation efficiency of NO at various jet velocities

With the increase of jet velocity, the oxidation efficiency of NO by ˙OH also increased (Fig. 8). At the jet velocity 3 m/s, the oxidation effect was very poor, and its efficiency was less than 40%. The oxidation efficiency still showed an upward trend in the second half of the pipeline. Considering that it was consistent with the entry speed of exhaust gas, there was no cluster effect, which may be due to insufficient contact range, and all oxidation processes cannot be completely completed within 10 s. When the jet velocity increased from 5 m/s to 8 m/s, the oxidation efficiency was still improved obviously. There was still no complete diffusion for the jet velocity 5 m/s, but when it was above 8 m/s, further increase of the jet velocity had a small effect on the oxidation efficiency. Overall, the jet velocity has a great influence on the oxidation of NO by ˙OH.

Effect of H_2O concentration. The inlet velocity of exhaust gas was 3 m/s, the concentration of NO 100 ppm, the molar fraction of carbon dioxide 12%, the molar fraction of oxygen 5%, the jet velocity 10 m/s, the temperature 473 K, the molar ratio of ˙OH/NO 1.4, N_2 was used as inert gas, the molar fraction of water in the waste inlet was changed, and the oxidation efficiency of ˙OH radicals by NO under various water contents was simulated. The measurement time was 10 s.

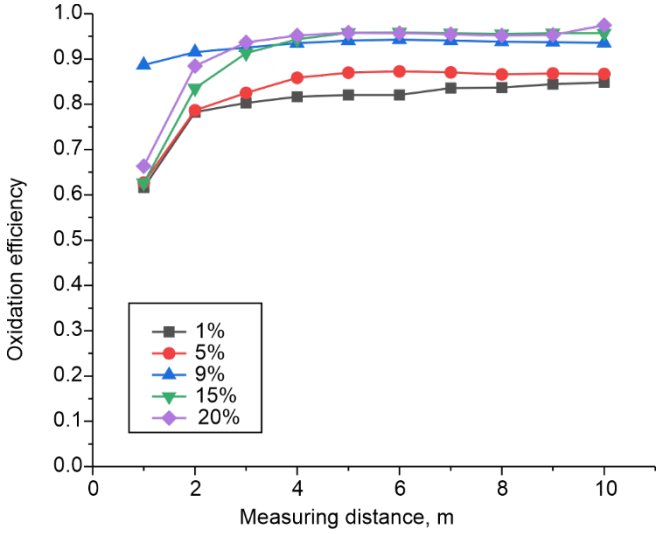

Fig. 9. Oxidation efficiency of NO at various H_2O concentrations

With the increase of water concentration, the efficiency of NO oxidation increases to a certain extent (Fig. 9). As results from the sensitivity analysis (Fig. 6), when the content of H_2O increased, the rate of reaction R58 to the right accelerated, the increase of the content of H_2O_2 indirectly promoted the formation of ˙OH radicals improving the oxidation efficiency of NO. However, when water concentration increases from 1% to 20%, the oxidation efficiency could be improved by about 10%. Compared with other influencing factors, water concentration has little influence on the oxidation efficiency of NO.

Effect of O_2 concentration. The inlet velocity of exhaust gas was 3 m/s, the concentration of NO was 100 ppm, the molar fraction of carbon dioxide was 12%, the molar fraction of water was 5%, the jet velocity 10 m/s, the temperature 473 K, the molar ratio of ˙OH/NO was 1.4, N_2 was used as inert gas, the molar fraction of oxygen at the inlet of exhaust gas were changed, and the oxidation efficiency of ˙OH by NO was simulated under various oxygen concentrations. The measurement time was 10 s.

In the range of 1–15% of oxygen mole fraction, the oxygen concentration had little effect on the efficiency of NO oxidation, and its efficiency fluctuated between 86% and 90% without obvious rule (Fig. 10). However, when the mole fraction of oxygen reached 21%, the oxidation efficiency of NO was obviously improved, and the efficiency was as high as 98.8%, which was close to the complete oxidation degree. It seems that in the Fenton reaction system, O_2 was a kind of intermediate that can capture ˙OH radicals. It blocks the collision reaction, reduces the annihilation of ˙OH radicals, and improves its utilization [22, 23].

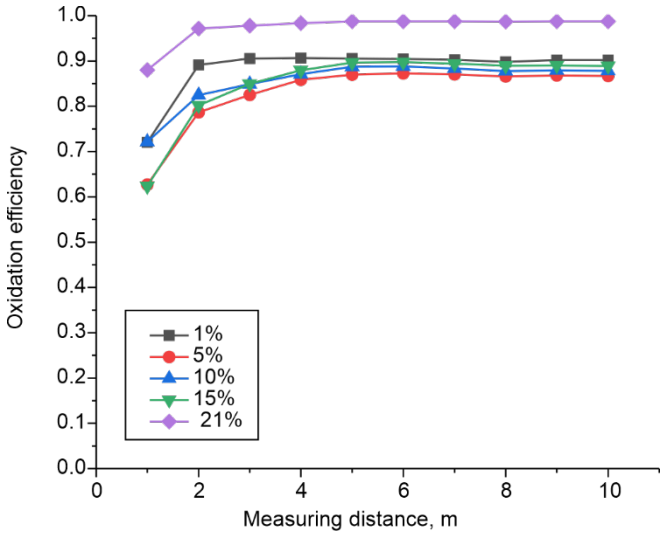

Fig. 10. Oxidation efficiency of NO at various O_2 concentrations

In the range of oxygen mole fraction from 1% to 15%, this capture effect was not obvious, so it has little effect on the oxidation efficiency of NO. When the mole fraction of oxygen reached 21%, the capture effect was greatly enhanced, so the oxidation efficiency of NO was significantly improved. However, compared with other influencing factors, oxygen concentration has little effect on NO oxidation efficiency.

4. CONCLUSIONS

- When the jet velocity exceeded the incident velocity of exhaust gas to play the role of shower, the oxidation efficiency was significantly improved compared with that without shower effect. The contents of water and oxygen had little effect on oxidation efficiency.
- Temperature and molar ratio of ˙OH/NO were the key factors affecting the efficiency of NO oxidation by ˙OH radicals. The best conditions for the oxidation of NO in flue gas should be at temperatures from 473 to 523 K, the molar ratio of ˙OH/NO should be maintained at about 1.4, the jet velocity sat 10 m/s, and the flue gas velocity at 3 m/s. Small fluctuations of the remaining factors in the actual flue gas have little effect on the overall oxidation efficiency.

ACKNOWLEDGEMENT

This research was supported by Zhejiang Provincial Key Research and Development Program (Grant No. 2020C03084).

REFERENCES

[1] SRIDAN P., SURAPOLCHAI P., *A system approach to biomass energy development. Thailand's path towards sustainable development*, ETA-Florence Renewable Energies, 2020, 786–797

[2] GUO D., *Acid rain and its harm*, J. Heilongjiang Water Science Institute, 2006, 1–5. DOI: 10.13524 /j.2095-008x.2006.02.001.

[3] NIU J., NIU D., ZHOU H., *Review on the harm of acid rain and its prevention and control*, J. Dis. Sci., 2008, 23 (4), 110–116.

[4] FANG X., *Harm and prevention of air pollution to agricultural production*, South. Agric. Mach., 2017, 48, 50–55.

[5] QI F., *Pollution and treatment of nitrogen oxides*, Jiangsu Build. Mater., 2016, 7–10.

[6] LIU X., *Based on the harm of nitrogen oxides and its prevention measures*, Low Carbon World, 2017, 9 (3), 8–9. DOI: 10.16844/j.cnki.cn10-1007/tk.2017.09.006. DOI: 10.16844/j.cnki.cn 10-1007/tk. 2017.09.006.

[7] JIN C.J., CHEN H.M., WANG L.Y., CHENG X.X., SUN R.F., *Adsorption and regeneration of volatile organic compounds (VOCs) on coal-based activated carbon by ferric nitrate modification*, China Petr. Proc. Petrochem. Technol., 2021, 23, 137–150.

[8] WANG Y., *Discussion on the application of SNCR flue gas denitration technology*, China El. Power Educ., 2010, S2, 455–456.

[9] HU J., *Study on the reaction mechanism of ZSM-5 supported Mn/Co-Al/Ce/Ti catalyzed SCR and rapid SCR*, Hangzhou Dianzi University, 2017, 6.

[10] SAMOJEDEN B., MOTAK M., GRZYBEK T., *The influence of the modification of carbonaceous materials Cross Mark on their catalytic properties in SCR-NH_3. A short review*, Compt. Rend. Chim., 2015, 18, 1049–1073. DOI: 10.1016/j.crci.2015.04.001.

[11] CHENG X.X., BI X.T.T., *A review of recent advances in selective catalytic NO_x reduction reactor technologies*, Partic., 2014, 16, 1–18. DOI: 10.1016/j.partic.2014.01.006.

[12] YANG J., MEI Y., WANG C., LONG G., LI S., *Current status and trends on wet flue gas denitration technology*, Chem. Ind. Eng. Progr., 2017, 36, 695–704. DOI: 10.16085/j.issn.1000-6613.2017.02.041.

[13] LIN S., *Research progress of simultaneous desulfurization and denitrification by liquid phase oxidation absorption*, Coal Chem. Ind., 2015, 43, 24–27.

[14] PAN J., DENG J., ZHANG Q., *Application progress of advanced oxidation technology of hydroxyl radical*, J. Guangdong University of Technology, 2019, 2, 70–77.

[15] BRILLAS E., GARCIA-SEGURA S., *Benchmarking recent advances and innovative technology approaches of Fenton, photo-Fenton, electro-Fenton, and related processes. A review on the relevance of phenol as a model molecule*, Sep. Purif. Technol., 2020, 237, 116337. DOI: 10.1016/j.seppur. 2019.116337.

[16] CUI R., MA S., WANG J., SUN S., *NO oxidation over Fe-based catalysts supported on montmorillonite K10, g-alumina and ZSM-5 with gas-phase H_2O_2*, Chemosphere, 2019, 234, 302–309. DOI: 10.1016 /j.chemosphere.2019.06.029.

[17] SONG Z., WANG B., YANG W., CHEN T., MA C., SUN L., *Simultaneous removal of NO and SO_2 through heterogeneous catalytic oxidation-absorption process using magnetic $Fe_{2.5}M_{0.5}O_4$ (M = Fe, Mn, Ti and Cu) catalysts with vaporized H_2O_2*, Chem. Eng. J., 2020, 386, 123883. DOI: 10.1016 /j.cej.2019.123883.

[18] WEN Z., SHEN H., LIU Y., HUANG Q., *Experimental study on the NO oxidation and removal by heterogeneous Fenton reaction*, J. Environ. Eng., 2022, 148 (1). DOI:10.1061/(asce)ee.1943-7870.0001963.

[19] PHAM A.L.T., LEE C., DOYLE F.M., SEDLAK D.L., *A silica-supported iron oxide catalyst capable of activating hydrogen peroxide at neutral pH values*, Environ. Sci. Technol., 2009, 43, 8930–8935. DOI: 10.1021/es902296k.

[20] LI H., WU J., LIU J., *Finite element mesh generation and mesh quality judgment index*, China Mech. Eng., 2012, 23, 368–377.

[21] WEN Z.C., LIU Y., SHEN H., XU J., *A theoretical study on the destruction of typical biomass tar components (toluene, phenol and naphthalene) by ˙OH radicals*, J. Indian Chem. Soc., 2021, 98, 100015. DOI: 10.1016/j.jics.2021.100015.

[22] MA S., MA J., ZHAO Y., *Experimental study on flue gas desulfurization and denitrification with UV/H_2O_2 system*, Proc. CSEE, 2009, 5, 27–31.

[23] LI L., GAO N., *Effect of anions on degradation of bisphenol A by UV/H_2O_2 microaeration process*, China Environ. Sci., 2008, 28, 4. DOI: 10.3321/j.issn:1000-6923.2008.03.009.

[24] HUANG Z., XIE X., *Energy revolution under vision of carbon neutrality*, Bull. Chinese Academy of Sciences, 2021, 2021, 36, 1010–1018. DOI: 10.16418/j.issn.1000-3045.20210812001.

[25] WEN Z.C., LIU Y., SHEN H.Z., DING N., LI Y., LUO D., *Mechanism and kinetic study on the degradation of typical biomass tar components (toluene, phenol and naphthalene) by ozone*, Ozone Sci. Eng., 2021, 43, 78–87. DOI: 10.1080/01919512.2020.1760077.